COMPACT IGNITION TOKAMAK PHYSICS AND ENGINEERING BASIS*

R.R. PARKER[1], G. BATEMAN, P.L. COLESTOCK,
H.P. FURTH, R.J. GOLDSTON, W.A. HOULBERG[2],
D. IGNAT, S. JARDIN, J.L. JOHNSON, S. KAYE,
C. KIERAS-PHILLIPS, J. MANICKAM,
D.B. MONTGOMERY[1], R. MYER[1], M. PHILLIPS[3],
R. PILLSBURY[1], N. POMPHREY,
M. PORKOLAB[1], D.E. POST, P.H. RUTHERFORD,
R. SAYER[4], J. SCHMIDT, G. SHEFFIELD,
D.J. SIGMAR[1], D. STOTLER, D. STRICKLER[4],
R. THOME[1], R. WEINER[5], J.C. WESLEY[6]
Plasma Physics Laboratory,
Princeton University,
Princeton, New Jersey,
United States of America

Abstract

COMPACT IGNITION TOKAMAK PHYSICS AND ENGINEERING BASIS.

The Compact Ignition Tokamak (CIT) is a high-field, compact tokamak design whose objective is the study of physics issues associated with burning plasmas. The toroidal and poloidal field coils employ a copper–steel laminate, manufactured by explosive-bonding techniques, to support the forces generated by the design fields: 10 T toroidal field at the plasma center; 21 T in the OH solenoid. A combination of internal and external PF coils provides control of the equilibrium and the ability to sweep

* Work supported by the United States Department of Energy Under Contract No. DE-AC02-76 CHO3073.

[1] Massachusetts Institute of Technology, Cambridge, MA, USA.

[2] Oak Ridge National Laboratory, Oak Ridge, TN, USA.

[3] Grumman Aerospace Corporation, Princeton, NJ, USA.

[4] Fusion Engineering Design Center, Oak Ridge National Laboratory, Oak Ridge, TN, USA.

[5] Max-Planck-Institut für Plasmaphysik, Garching bei München, Federal Republic of Germany.

[6] General Atomics Inc., San Diego, CA, USA.

the magnetic separatrix across the divertor plates during a pulse. At temperatures and β_α levels characteristic of ITER designs, the fusion power in CIT approaches 800 MW and can be the limiting factor in the pulse length. Ignition requires that the confinement time exceed present L-mode scalings by about a factor of two, which is anticipated to occur as a result of the operational flexibility incorporated into the design. Conventional operating limits given by $\langle\beta\rangle < 3I/aB$, $\bar{n}_{20} < 2B/Rq_e$ and $q_\psi \leq 3.2$ have been chosen and, in the case of MHD limits, have been justified by ideal stability analysis. The power required for CIT ignition ranges from 10 MW to 40 MW or more, depending on confinement assumptions, and either ICRF or ECRF heating, or both, will be used.

1. Introduction

The objective of the CIT project is to explore the "physics of burning plasmas" within the parameter range of interest for the operation of D-T tokamak reactors. The use of a high-field tokamak for this task offers important economies, but is subject to experimental constraints associated with the magnitude of the fusion-power density. The CIT design approach favors operation in enhanced-confinement regimes, so as to relieve the fusion heat-load problem, while providing a generally useful model for tokamak reactors.

Single-alpha-particle phenomena (such as orbital excursions, classical slowing-down and transport by bulk-plasma fluctuations) are being addressed effectively by the TFTR-JET generation of fusion-plasma experiments [1,2]. Burning-plasma operation in ITER and more advanced fusion reactors [3,4] will involve the combination of two distinctive new types of plasma-physical phenomena:

(1) alpha-particle-driven instability modes (fishbones, Alfvén waves, MHD modes, trapped-particle modes), along with related stabilizing effects;

(2) fusion-heat-driven thermal excursions (sawteeth, loss of plasma-temperature control).

The CIT experiment is designed to study these two new types of burning-plasma phenomena and their interactions, with particular emphasis on providing relevant information for D-T operations in ITER.

The alpha-plasma-physics phenomena [5] [type (1)] depend on local plasma parameters such as n_α/n_e, β_α, β_{th}, and $v_\alpha/v_{Alfvén}$ – not on global parameters such as τ_E. Figure 1 provides a "universal plot" of the effective alpha-heating-power density $p_\alpha^* = p_\alpha - p_{Brems}$ and the characteristic alpha-plasma-physics parameters as functions of n_e/B^2 and T.

For tokamak reactors, efficient quasi-steady-state operation (very high electrical conductivity and/or noninductive current drive) will set a minimum operating-temperature requirement of order $T(0) \gtrsim 20$ keV, so that the reactor-relevant range of central n_α/n_e-values lies above 0.7%. The relevant levels of β_{th} and β_α are determined by the desired fusion power-density. For example, for $T(0) \gtrsim 20$ keV, an ITER requirement of $\langle p_f \rangle = 5 \langle p_\alpha^* \rangle \gtrsim 1.5$ MW m^{-3} at $B = 5$ T, corresponds roughly to $\beta_{th}(0) \gtrsim 10\%$ and $\beta_\alpha(0) \gtrsim 2\%$ in Fig. 1.

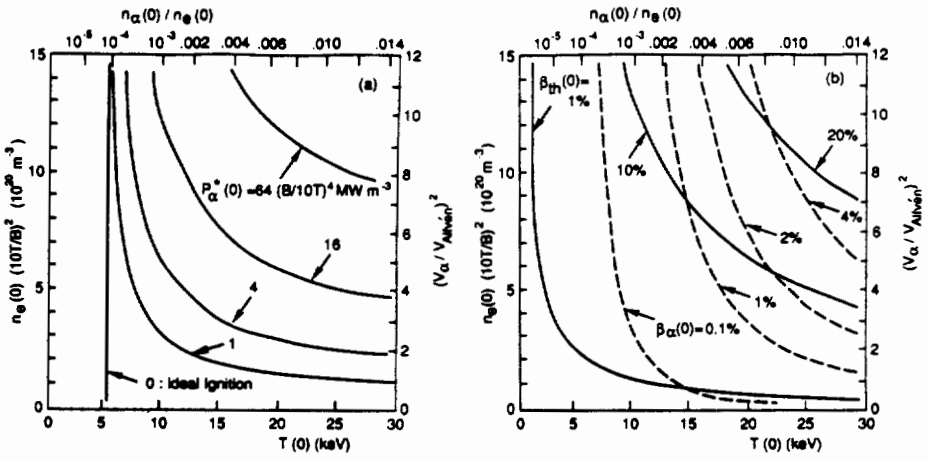

FIG. 1: (a) Fusion power density for thermal D-T plasmas with a carbon impurity level of $Z_{eff} = 1.5$; (b) characteristic alpha-plasma-physics parameters. For the profiles $T = T(0)\ (1 - r^2/a^2)$ and $n = n(0)\ (1 - r^2/a^2)^{1/2}$, where r is radial distance from the magnetic axis in the equatorial plane, volume-averaged quantities are given by $\langle T \rangle = 1/2\ T(0)$, $\langle n \rangle = (2/3)\ n(0)$ and $\langle \beta_{th} \rangle = (2/5)\ \beta_{th}(0)$. When $T(0) \gtrsim 20$ keV, we have $\langle p_\alpha^* \rangle \sim 0.3\ p_\alpha(0)$, and a total CIT fusion power of $P_f \sim 50$ m$^3\ p_\alpha^*(0)$.

The ability of high-field burning-plasma experiments like CIT to investigate reactor-relevant plasmas is constrained by heat-deposition problems. Figure 1 shows that for $B = 10$ T the magnitude of $p_\alpha^*(0)$ associated with $\beta_\alpha(0) = 1$–2% falls roughly into the range between the 4 and 16 MW m^{-3} curves, (corresponding to total CIT fusion powers of about 200-800 MW). Special divertor techniques will be used in CIT (cf. Sec. 4) to maximize the finite-β_α operating window at the 10 T level by distributing the heat-outflow, but the development of an enhanced-confinement regime that burns at lower field strength would give valuable relief by reducing p_α^* in proportion to B^4 for a specified magnitude of β_α.

Fusion-heat-driven plasma phenomena [type (2)] do not depend on the parameters of the alpha-particle population, but depend rather on the characteristics of the global heat-flow pattern. Fusion-driven thermal excursions can arise on the high-temperature side of the Cordey pass (Fig. 3, Sec. 3), where the Q-value is only 5-10, but where the destabilizing term $d \log Q/d \log T$ becomes large. For tokamak reactors, where stable transit through the Cordey pass can be assured by controlling the auxiliary heating power, the key issue is the degree of stability of the high-temperature, high-Q equilibrium-burn point against perturbations that may cause collapse of the burn, followed by disruption of the tokamak discharge. To permit study of the relevant stability phenomena, the CIT experiment aims at producing extended equilibrium-burn pulses in the $T(0) \gtrsim 20$ keV regime. For 10 T operation, the time-averaged fusion-power in this regime should be kept within the 600 MW level (*i.e.*, somewhat below the 16 MW m^{-3} curve in Fig. 1), to allow the burn-length to approach the magnetic-field flat-top time of ~ $10\tau_E$. If enhanced confinement permits 7 T operation, the fusion power for a given β_α is reduced by a factor of 4, and the flat-top time is extended to $\gtrsim 20\ \tau_E$.

The remainder of this paper describes the engineering design of CIT and various aspects of the physics basis. Section 2 gives a brief description of CIT engineering aspects and construction plans. Section 3 summarizes CIT physics in the areas of confinement and transport analysis. Section 4 presents axisymmetric MHD design, while Section 5 describes MHD stability considerations. Section 6 summarizes the plans for auxiliary heating.

2. CIT Engineering Design

The CIT device core, shown in Fig. 2, is in the preliminary design phase. In order to achieve its mission in a cost-effective manner, the CIT is being designed as a compact, high-field tokamak with a major radius of 2.1 m (Table I). The maximum field on axis is specified as 10 Tesla for 3000 pulses, and 11 Tesla for a reduced number of pulses.

The 20-coil toroidal field (TF) system uses pure wedging to react the centering force. Wedging has several advantages relative to bucking against a center post, including greater ability to resist out-of-plane loads in the TF inner leg, superior predictability of interface conditions, and a simpler mechanical structure, which can be tested prior to installation.

In order to achieve the desired parameters within the TF design envelope, an explosively bonded laminate of copper and Inconel is used as the conductor material. The properties of the laminate, which are determined by the high conductivity of copper at LN_2 temperatures and the high strength of the Inconel, are superior to the properties of other available conductor options. The TF and PF coil systems are LN_2 cooled between pulses, to allow high current density and low resistive energy consumption.

TABLE I
CIT PARAMETERS AND OPERATIONAL LIMITS

PARAMETERS	BASELINE[a)]
Major Radius	2.1 m
Minor radius	0.65 m
Aspect Ratio	3.25
Elongation (95% surface)	2.0
Field on Axis	10 T
Current @$q = 3.1$	11 MA
Neutron wall loading	
@ 0.8 beta limit	6.0 MW/m^2
TF Flat-top time	5 sec
Energy/Peak Power	
7 T, 7.7 MA	6.2 GJ/600 MW
10 T, 11 MA	11.9 GJ/1300 MW

a) A larger vacuum vessel alternative is also under study which would allow 13 MA currents. A limited number of 11 T discharges is also possible.

PLASMA OPERATIONAL LIMITS

Normalized Beta, $\beta(\%)/(I/aB)$	3.0
Elongation, κ	2.0
Normalized Density, $\bar{n}_{20}/(B/Rq_e)$	2.0
Safety Factor, q_ψ	3.2 (min)
Triangularity, δ	0.25 (min)

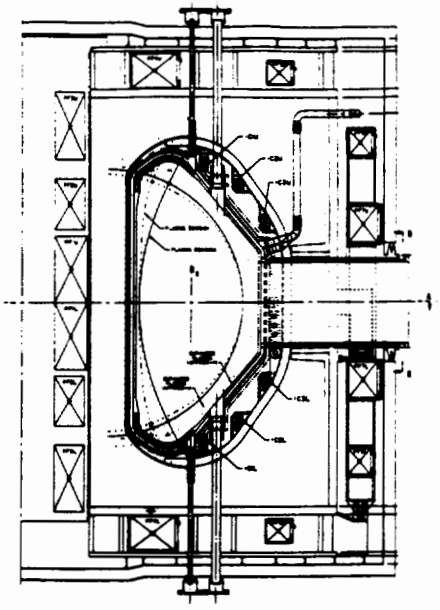

FIG. 2: Elevation view of the Compact Ignition Tokamak. During the flat-top, the equilibrium is swept between the two extremes shown, in order to distribute the heat flow on the divertor plates.

The poloidal field (PF) coil system, is composed of 7 up/down-symmetric pairs of independently controlled coils located outside the toroidal field (TF) coils and 3 pairs of smaller control coils located inside the TF coils, but outside the vacuum vessel. The coils of the central solenoid, like the TF coils, use copper-Inconel laminate as the conductor material, because of the high stresses associated with producing fields up to 21 T. The internal coils are required to provide vertical stability and fast radial control, while the external coils provide

the ohmic-heating, equilibrium, and shaping fields, including those needed for divertor sweeping.

The vacuum vessel is a solid-wall Inconel-625 weldment. It will be fabricated in two 180° segments consistent with the two half-machine assemblies of TF coils. The halves will be brought together and the final two welds accomplished to complete the assembly. The wall will be protected by a tile system. Pyrolytic graphite will be used for the divertor plates, carbon/carbon composites for the limiter, and bulk graphite tiles for the remaining areas. The horizontal access is by 20 ports of 38 cm × 100 cm. Vertical access is more limited, consisting of 5 cm and 10 cm tubes.

Internal remote maintenance will be accomplished using two articulated boom manipulators, each servicing half the vacuum vessel interior from a storage cask permanently attached to one of the horizontal ports in each 180° segment. Remote maintenance within the test cell (machine exterior) is presently envisaged as using servo-manipulators on a crane-mounted boom. The primary functions of the remote-maintenance systems are: first-wall inspection and repair, vacuum vessel and port-welding repair, diagnostic repair and replacement, and coolant, power, and instrumentation lead repair. Major machine repair is not part of the remote maintenance mission.

Initial operation of CIT at 7.0 T will be powered by a combination of the existing TFTR motor-generator-flywheel units and an additional 2 GJ from the existing 138 kV service, with minimal modifications. The energy will be converted by the existing TFTR convertors with modifications that take advantage of the low CIT pulse repetition rate to improve their pulse-load capacity. When performance at the 10-11 T level is required, additional energy will be provided either by full exploitation of site-utility pulse-load capacity, or by installation of additional motor-generator units.

3. Confinement Analysis

3.1. Global Projections

CIT performance has been projected using a variety of empirically-determined confinement models, ranging from neo-Alcator scaling, which corresponds to ohmic confinement for regimes in which τ_E is not saturated with density, to Goldston scaling [6], which yields a good fit to most confinement data from neutral-beam heated, present-day tokamaks operating in the L-regime. For those models in which τ_E does not degrade explicitly or implicitly with power, for example neo-

Alcator or ASDEX-H, CIT ignites easily; attention has therefore been focused on evaluating the operating regimes permitted by power-degrading models in which the total power, as given by the sum of ohmic, auxiliary and α-particle contributions, is used. The operational limits assumed for these analyses are the Hugill-Murakami density limit, $\bar{n}_{20} \leq 2B/Rq_e$, where $q_e = 5a^2\kappa B/RI$, the Troyon-Gruber beta limit $\beta \leq 0.03\ I/aB$, and $q_\psi > 3.2$. The profiles are of the form $X = x(0)(1 - r^2/a^2)^{\nu_x}$, where r is radial distance from the axis in the equatorial plane and concentric, elliptical flux-surfaces with constant ellipticity are assumed.

Projections based on power-degrading confinement models are more pessimistic than for non-power-degrading models, and an ignition window requires an enhancement factor which depends on the density profile. Figure 3 shows the ignition window for a recent

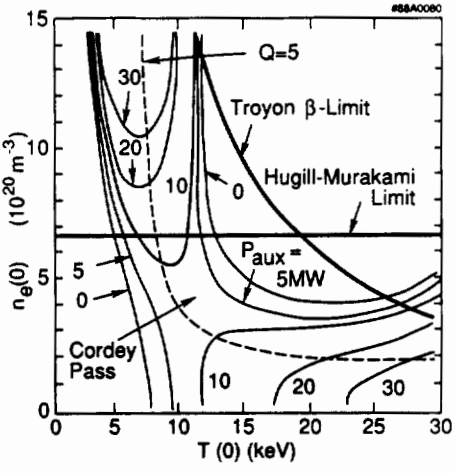

FIG. 3: POPCON diagram of auxiliary-heating power requirements for CIT, with parameters $B = 10$ T, $Ip = 11$ MA, and temperature and density profiles as in the Fig. 1 caption. Classical and neo-Alcator transport are assumed, plus Kaye "big tokamak" transport ameliorated by a factor of 2. The Hugill-Murakami density limit, Troyon beta limit, and $Q = 5$ curve are indicated.

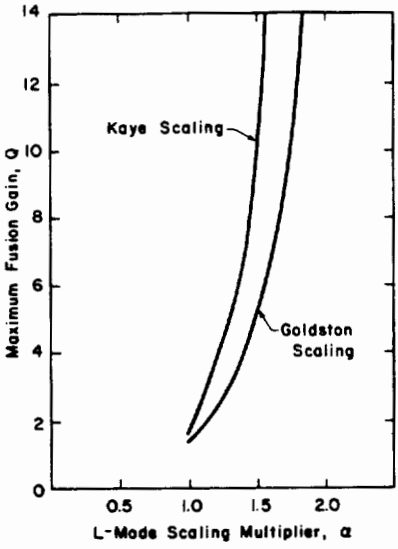

FIG. 4: Thermonuclear power gain in CIT as a function of L-mode-scaling multiplier $\alpha_L = \tau_E/\tau_L$ where τ_L is the L-mode confinement time. The two curves shown are for τ_L given by Goldston [6], corrected for mass effects, and Kaye [7].

empirical scaling due to Kaye [7], where an enhancement factor of 2 has been used. With an enhancement factor of 1.3-1.7, depending on the L-mode model used, high-Q (5–10) operation is still obtained (Fig. 4), using the relatively flat density-profiles corresponding to $\nu_n = 1/2$. More strongly peaked density-profiles require a smaller enhancement factor.

Several measures have been adopted to improve performance relative to L-mode projections. These include the combination of enhanced confinement and decreased ignition requirements resulting from peaking of the density profile by pellet fueling and control of recycling, the possibility of improved confinement by operating with a properly designed divertor (H-mode), and the improvement in effective confinement owing to the peaked energy-deposition-profiles associated with ICRH, ECRH and alpha heating [8]. The prospects of achieving the required confinement in CIT using one or more of these techniques are good, considering confinement results in present-day large tokamaks. For example, enhancement factors of 2 or more are now reliably obtained in both TFTR (supershots) and JET (H-modes). However, even for the limiting case of pure L-mode scaling, CIT has the potential option of increasing the current to 12-14 MA, which would provide adequate Q-values (~ 5) to permit meaningful alpha-heating studies.

3.2. Transport Studies

Optimum performance in time-dependent simulations of CIT [9] is achieved with the following scenario: the toroidal field, plasma current and shape are ramped simultaneously in order to aid current penetration while avoiding a broad sawtooth mixing region that would spread out the density and temperature profiles [10]. A succession of pellets are injected during this ramp-up while the plasma energy density is low enough to allow pellet penetration. Deeply penetrating pellets produce centrally peaked density profiles and inhibit broad sawtooth oscillations [11]. While the deuterium and tritium density profiles are still centrally peaked, the plasma is heated to produce central ion temperatures above 10 keV. In this scenario, sawteeth need to be delayed or kept small until after ignition, because the steady-state sawtooth-mixing radius (after magnetic diffusion) is predicted to cover about half the plasma in the elongated geometry of CIT.

When a Kadomtsev sawtooth model is used to simulate the presence of broad sawteeth, it is found that short-wavelength ideal-MHD ballooning modes are unstable within the sawtooth-mixing region during each reheat cycle of the sawtooth oscillation. However, if

the current density (and magnetic flux) is only partially redistributed during each sawtooth crash, so that the q-value on axis remains well below unity, as observed in Faraday-rotation measurements on several tokamaks [12,13], then our simulations indicate that the magnetic shear remaining within the sawtooth-mixing region stabilizes high-n ideal ballooning modes during most of the sawtooth rise, even with large-amplitude (20 – 30 keV) sawteeth after ignition. The strong central peaking of the current profile induced by neoclassical resistivity is an essential feature of this model.

4. Axisymmetric MHD Design and Analysis

Nominal PF-coil current waveforms during the current ramp-up, flat-top and current ramp-down phases of CIT have been obtained using the static free-boundary equilibrium and optimization code, VEQ, and the dynamic equilibrium and transport simulation code, TSC. At certain critical times, which bracket significant changes in plasma shape and/or beta (*e.g.*, start of flat-top, end of burn, etc.), the VEQ code is used to determine PF-coil currents for MHD equilibria with assumed plasma profiles, flux linkages, and prescribed values of the major and minor radius, and the positions of the inboard and outboard divertor strike-points. The solutions are additionally constrained to minimize the coil energy $W_{pf} = 1/2\, I^t M I$, where $I^t = [I_{PF1}, \ldots, I_{PF7}]$. Detailed calculations of the plasma evolution during a complete discharge scenario are provided by the TSC code. This free-boundary axisymmetric simulation code includes a 2-D transport description of an auxiliary-heated D-T plasma. Circuit equations couple the plasma to time-varying currents in the poloidal field coils and eddy currents in the vacuum vessel and TF support structure. Pre-programmed PF-current waveforms supplied by VEQ are feedback-adjusted to be made compatible with the transport-generated profiles, and a detailed accounting of the volt-second consumption is obtained. The plasma-shape history is chosen to ensure satisfactory q-edge evolution from the viewpoint of MHD stability considerations. Appropriate shaping of the plasma during the current ramp-up, aided by simultaneous ramping of the toroidal magnetic field, also assists current penetration into the plasma. Figure 5 shows snapshots of the calculated plasma shape at various times during one TSC simulation. The plasma is grown from the outboard limiter and becomes diverted at $t = 6.5$ sec. During the current flat-top, the divertor separatrix is swept in the direction of increasing triangularity, to alleviate the heat loads on the divertor plates.

The axisymmetric vertical instability of the CIT plasma is a critical issue that has received extensive investigation. Computations using TSC show that the vacuum vessel and TF support structure have time

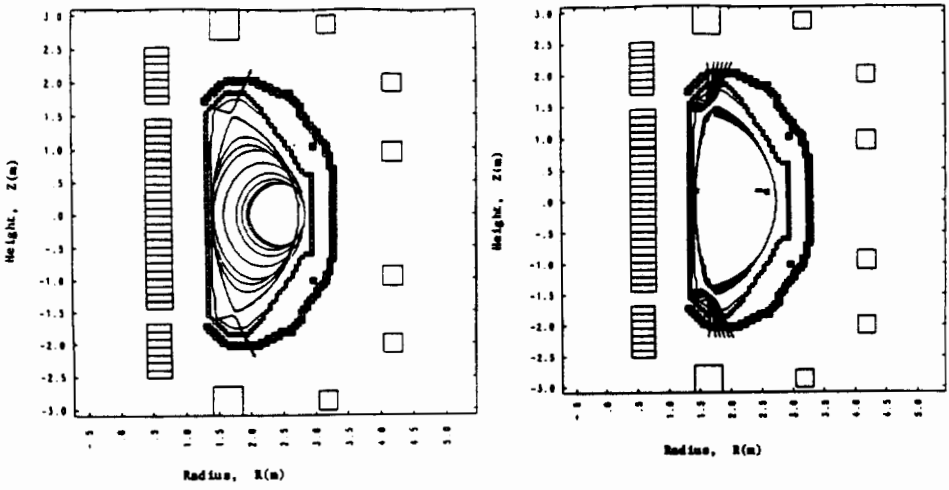

FIG. 5: Snapshots of plasma shape at various times during the current ramp (left), and current flattop (right). The programmed divertor sweep during the flattop phase is clearly seen.

constants of approximately 16 msec and 40 msec, respectively, providing effective passive vertical stabilization of the plasma. The maximum growth rate for the instability (8.3 msec) occurs during the current flat-top. To effect complete vertical position control, a two-level PID feedback-control system has been used, similar to that proposed for the ASDEX-U experiment. Such a two-level system decreases the effective L/R time of the feedback circuit. In the first level of the feedback, currents in the internal control coils respond to the measured deviation of the magnetic axis position from the midplane. In the second level, the PID system responds to the deviation of the desired feedback currents from the actual currents. The effect of time delay in the feedback circuit has also been considered, and the limiting delay for which vertical feedback control could be maintained was found to be 3.5 msec.

The poloidal-field control system is designed to control the plasma position and shape on several different time scales. On the fastest time scale, $t < 10$ msec, the vacuum vessel provides passive control. Over slightly longer times, $10 < t < 100$ msec, the internal control coils control the plasma. Each of these coils is capable of $\pm$ 800 kA with $\pm$ 80 V/turn. Over times longer than 100 msec, the main PF coils external to the TF are able to relieve the internal coils and assume control. Calculations have shown that, if the plasma poloidal beta decreases abruptly by 0.3, the two-time control system can limit the radial excursion of the plasma to 3 cm.

Simulations of radial and vertical plasma disruptions have been performed that provide time histories of induced vacuum-vessel currents for detailed engineering load and stress analyses. A disruption is initiated at some chosen time by enhancing the plasma thermal conductivity by some factor. The consequences of plasma current decay rates of up to 3.5 MA/msec have been investigated. The most extreme forces on the vacuum vessel are found to result from simulations where loss of vertical-position control occurs prior to the current quench. For a vertical disruption with a current-quench rate of 3.4 MA/msec occurring after a vertical displacement of 45 cm, an extreme net inward radial force of 11.9 MNt/radian is obtained. These loads are used to design the vacuum chamber thickness and its support system.

5. Non-axisymmetric MHD Stability

An extensive theoretical survey of the geometric factors (aspect ratio, ellipticity, and triangularity) shows that there is a broad window in parameter space, within which MHD-stable plasmas can be maintained. This favorable window exists for ellipticities up to about 2, provided that the triangularity is moderately large (about 0.5). At larger values of ellipticity or triangularity, there are complex interactions between the role of the configuration shape and the plasma current profiles, which can result in strong instabilities, both internal and external. The CIT shape parameters have been chosen to lie within the favorable window.

The stability limits depend strongly on the pressure distribution and the q profile. Since q-conserving sequences with increasing β lead to finite current at the plasma edge, most of the studies have employed an ohmic constraint to relate the parallel current density to the temperature. An arbitrary density profile can be used to decouple the pressure and temperature profiles. Prescribing the pressure distribution so that the plasma is marginally stable everywhere to ballooning modes provides reasonable configurations with good stability properties. The critical β is usually determined by infinite-n ballooning modes in systems with a peaked current profile. For broad current profiles, low-n kink modes are more restrictive [14].

The behavior of the low-n kink modes, which determine $\beta_{critical}$ in systems with broad current distributions, is very sensitive to the shape of the current profile near the edge, especially if $q_{95\%} \lesssim 3$. Drops in the value of $C_T = \langle\beta\rangle/(I/aB)$ occur when low-order rational surfaces lie near the plasma edge. The "infernal mode", a pressure-driven low-n internal instability, tends to be most limiting if the pressure profile is not

coupled to the q-profile through a ballooning criterion. Such modes restrict operation to low values of C_T whenever there is a significant pressure gradient in a region with little shear, especially if $q(0) \approx 1$.

Stability studies have been made for pressure and current profiles obtained from self-consistent simulations of a CIT discharge. The results are very sensitive to the model employed to represent the behavior of the plasma during a sawtooth relaxation. For a case where the current profile flattens completely during the sawtooth but α-particle heating quickly establishes a pressure gradient in this region, the value of $q(0)$ would have to be raised to about 1.05 for the plasma to remain stable, as can be seen in Fig. 6a. Less severe models of the sawtooth behavior provide reasonable sequences of stable equilibria. In particular, high-β operation is permitted for $q(0) < 1$ with sufficient triangularity, provided sawteeth do not occur to eliminate shear in the central region (Fig. 6b).

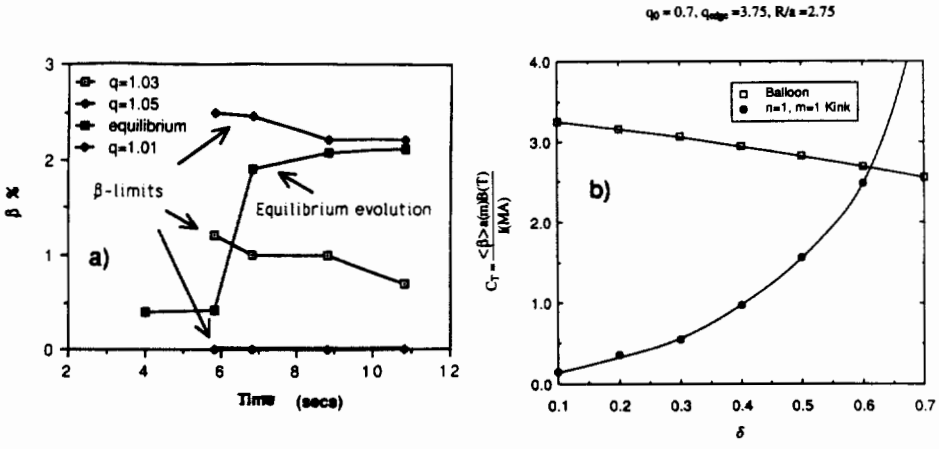

FIG. 6: a) Stability analysis of a TSC simulation of a CIT discharge, where a Kadomtsev reconnection, such that the q-profile is completely flattened inside the $q = 1$ surface, occurs 6 seconds into the discharge. The equilibrium evolution predicted by the code is shown by the open squares. The $\beta = 0\%$ results are imposed by internal modes in the shearless region if $q_0 = 1.01$. Increasing q_0 to 1.03 raises the β-limit to about 1%, and increasing it to 1.05 raises the stability limit to values above what the equilibrium evolution would predict. b) Effect of triangularity on C_T for non-sawtoothing discharges.

6. Auxiliary Heating

6.1. Ion Cyclotron Heating

An initial 10 MW of ICRF power, chosen primarily for its ability to deposit heating power locally in high-density plasmas, is planned for

CIT. The chief issues of importance in the design of such a system are (i) the choice of frequency of the heating mode, (ii) the plasma absorptivity, including the possibility of ramping the toroidal field during the rf pulse, (iii) equilibration rates of rf-induced fast ions, and (iv) coupling methods.

The heating mode chosen is minority heating, either He^3 minority in a full-field D-T plasma or H minority in a 2/3-field plasma, owing to its high absorptivity and proven heating efficiency in past experiments. In addition, the use of He^3 heating in the D-T mode permits the tritons to receive the deposited rf power directly, once their beta is sufficiently high, near ignition conditions. At CIT densities, the single-pass absorption rates are expected to be high, even as the toroidal field is ramped by 20% during the pulse. Some degradation in heating efficiency is expected during the ramp phase due to the non-central power deposition; however, the time required to reach ignition at flat-top is significantly shortened by this technique.

Due to the high densities involved, little or no fast ion tail is expected to be induced by the ICRF. Since the inter-species equilibration times are so short, ignition conditions may be approached by heating either electrons or ions. Indeed, direct electron heating is expected to occur as the electrons follow the ion temperatures toward ignition.

Coupling to the waves is planned through conventional inductive loops, which, however, are recessed from the vacuum vessel surface for protection. Two current straps are planned for each antenna cavity, to provide spectral control, consistent with experience in large tokamak experiments. The primary issues for the design of suitable antennas are (i) the maintenance of good rf coupling while providing protection from the edge plasma, (ii) the handling of thermal, mechanical and radiation loads on the antenna, and (iii) minimization of impurity influx while maximizing the delivered rf surface power density.

6.2. Electron Cyclotron Resonance Heating

Recent advances in high-frequency microwave source technology [gyrotrons or FEL's] make possible a serious consideration of electron cyclotron heating of CIT to ignition. If successful, ECRF technology may provide part or all of the required heating power in CIT. Because thermal equilibration between electrons and ions is much shorter than the expected energy confinement time at the high densities of interest, there is no significant difference between electron versus ion heating. ECRF has the advantage of power transmission

with the highest average power density among all RF technologies ($P/A \gtrsim 100$ MW/m^2).

Wave launching from the outside, possibly using quasi-optical transmission techniques, appears to be the most favorable under ignited plasma conditions. Altering the incident beam path may be achieved conveniently by simple reflecting mirrors. Single-pass absorption at the fundamental (280 GHz for $B = 10$ T) is achieved by injecting linearly polarized radiation with $\vec{E}_{RF}$ parallel to $\vec{B}_0$ (O-mode polarization) in which case good accessibility is expected up to a maximum density of $n(0) \simeq 8 \times 10^{20}$ m^{-3}. If operation at even higher densities were desired, second harmonic ($f = 560$ GHz) heating would allow good wave penetration and absorption up to $n \simeq 1.6 \times 10^{21}$ m^{-3} (X-mode) and $n \simeq 3.2 \times 10^{21}$ m^{-3} (0-mode). Because of the expected localized absorption, ECRH is particularly well suited for controlling MHD activity (sawteeth and disruption control) as well as improving confinement (H-mode production) [15].

Recent theoretical studies have concentrated on optimizing the wave-launching geometry (angles of incidence) for realistic CIT equilibria, as the on-axis magnetic field is raised from 8.0 to 10.0 Tesla. Ray tracing and absorption calculations have been carried out using the Livermore TORCH code for non-normal (relative to $\vec{B}$) angles of incidence [16]. For normal angles of incidence at $f \simeq f_{ce}$ a simplified absorption package, using the Bornatici relativistic absorption formula was used [17]. In this latter case good central absorption is ensured by noting that in the relativistic formulation there are no resonant particles which could absorb RF power from the incident waves on the low-field side of the resonant layer. The results of these studies, using a single frequency ($f = 280$ GHz) and outside O-mode launch, may be summarized as follows. By continuously varying the angle of injection from 30° off the normal at startup conditions [$B(0) = 8.0$ T, $T_e(0) \gtrsim 5$ keV, $n_e(0) \sim 2 \times 10^{20}$ m^{-3}, $\beta = 0.44$ %] to 0° (normal incidence) at full field [$B(0) = 10.0$ T, $T_e(0) = 10$ keV–20 keV, $n_e(0) = (1–8) \times 10^{20}$ m^{-3}] efficient single-pass central absorption is achieved through the post burn phase, as beta is varied in the range $\beta = (0.44–2.4$ %). With proper design, the power is absorbed within $r/a \lesssim 0.25$ for the full range of plasma parameters quoted. These results suggest that a single frequency may be sufficient for ECRF heating of CIT, with the field in the range 8-10 T.

References

[1] STRACHAN, J., *et al.*, Paper IAEA-CN-50/A-IV-5, this conference.

[2] JARVIS, O., *et al.*, Paper IAEA-CN-50/A-IV-4-2 (c), this conference.

[3] TOMABECHI, K., *et al.*, Paper IAEA-CN-50/F-I-4, this conference.

[4] BAKER, C. C., *et al.*, Nuclear Engineering and Design **63** (1981) 199-231.

[5] SIGMAR, D. J., Physica Scripta **T 16** (1987) 6.

[6] GOLDSTON, R., Plasma Phys. Controll. Fusion **26** (1984) 87.

[7] KAYE, S., Survey of energy confinement scaling, ITER Specialists Workshop on Energy Confinement, Max-Planck-Institut für Plasmaphysik, Garching bei München, Federal Republic of Germany, May, 1988, personal communication.

[8] CALLEN, J. D., CHRISTIANSEN, J. P., CORDEY, J. G., THOMAS, P. R., THOMASSEN, K., Nucl. Fusion **27** (1987) 1857.

[9] STOTLER, D. P., BATEMAN, G., Time-dependent simulations of a compact ignition tokamak, Rep. PPPL-2510, Princeton Plasma Physics Laboratory (1988). To appear in Fusion Technology.

[10] STOTLER, D. P., BATEMAN, G., Sawtooth effects in elongated, high current tokamak reactors, Rep. PPPL-2463, Princeton Plasma Physics Laboratory (1987). Fusion Technology, in press.

[11] BATEMAN, G., Delaying sawtooth oscillations in the compact ignition tokamak, Rep. PPPL-2373, Princeton Plasma Physics Laboratory (1986). To appear in Fusion Technology.

[12] SOLTWISCH, H., *et al.*, Current density profiles in the Textor tokamak (in *Plasma Physics and Controlled Nuclear Fusion Research 1986*, IAEA, Vienna) Vol. 1 (1987) 263–272.

[13] WEST, W. P., THOMAS, D. M., DeGRASSIE, J. S., ZHENG, S. B., Phys. Rev. Lett. **58** (1987) 2758.

[14] PHILLIPS, M. W., TODD, A. M. M., HUGHES, M. H., MANICKAM, J., JOHNSON, J. L., PARKER, R. R. To be published in Nucl. Fusion.

[15] LOHR, J., *et al.*, Phys. Rev. Lett. **60** (1988) 2630.

[16] SMITH, G. R., NEVINS, W. M., COHEN, R. H., KRITZ, A. M., Bull. Am. Phys. Soc. **31** (1986) 1516.

[17] BORNATICI, M., CANO, R., DeBARBIERI, O., ENGELMANN, F., Nucl. Fusion **23** (1983) 1153.